

# On the Application of Structured Sparse Model Selection to JPEG Compressed Images

Giovanni Maria Farinella and Sebastiano Battiato

Image Processing Laboratory,  
Dipartimento di Matematica e Informatica,  
Università degli Studi di Catania,  
Viale A. Doria 6 - 95125 Catania, Italia  
{gfarinella,battiato}@dmi.unict.it  
<http://iplab.dmi.unict.it>

**Abstract.** The representation model that considers an image as a sparse linear combination of few atoms of a predefined or learned dictionary has received considerable attention in recent years. Among the others, the Structured Sparse Model Selection (SSMS) was recently introduced. This model outperforms different state-of-the-art algorithms in a number of imaging tasks (e.g., denoising, deblurring, inpainting). Despite the high denoising performances achieved by SSMS have been demonstrated, the compression issues has been not considered during the evaluation. In this paper we study the performances of SSMS under lossy JPEG compression. Experiments have shown that the SSMS method is able to restore compressed noisy images with a significant margin, both in terms of PSNR and SSIM quality measure, even though the original framework is not tuned for the specific task of compression. Quantitative and qualitative results pointed out that SSMS is able to perform both denoising and compression artifacts reduction (e.g., deblocking), by demonstrating the promise of sparse coding methods in application where different computational engines are combined to generate a signal (e.g., Imaging Generation Pipeline of single sensor devices).

**Keywords:** Sparse Coding, Inverse Problems, Compression, Denoising, Image Enhancement, Image Restoration.

## 1 Introduction and Motivations

Many imaging issues require to solve an inverse problem, that is, the problem of estimating an image  $\mathbf{I}$  from a degraded version  $\mathbf{J}$  which has been obtained through a non-invertible linear degradation operator  $\mathbf{U}$ , and further altered by an additive noise  $\mathbf{w}$ :

$$\mathbf{J} = \mathbf{UI} + \mathbf{w} \quad (1)$$

Typical inverse problems in the context of image enhancement and restoration are *Denoising* (where  $\mathbf{w}$  is the Gaussian white noise and  $\mathbf{U}$  is neglected), *Deblurring* (where  $\mathbf{U}$  is a convolution operator and  $\mathbf{w}$  is the noise),

*Inpainting*<sup>1</sup> (where  $\mathbf{U}$  is a binary mask on the image and  $\mathbf{w}$  is typically neglected) and *Zooming* (where  $\mathbf{U}$  is a subsampling operator on a uniform grid and  $\mathbf{w}$  is typically neglected).

Among the methods used to address the above inverse problems [1–8], sparse coding has been receiving considerable attention as it has shown promising results [9–16]. Sparse coding is a method for modeling signals as sparse linear combinations of dictionary elements [17–19]. The basic assumption of this model is that natural images admit a sparse decomposition in some redundant basis (or so-called dictionary). Each image patch is considered as a discrete array of positive numbers that can be generated by linear combinations of overcomplete bases set, where the natural statistics are captured by the fact that the vector of coefficients is sparse, so that to generate the image patch only few bases contribute. Image enhancement and restoration is performed through estimation of the sparse coefficient vectors, related the overcomplete bases set under consideration, which are useful to approximate the original image patches from the degraded version.

Despite sparse coding have been tested on different image enhancement problems, literature lacks of studies on application of sparse coding in presence of lossy compression or in general when unknown (or partially known) degradation processes have been applied simultaneously. This motivates the study reported in here.

The lossy compression process (i.e., JPEG compression [20]) attempts to eliminate redundant or unnecessary information. High compression factor could badly influence the quality of the final images highlighting undesirable effects. Block-based coding, as in JPEG-compressed images, may produce a number of artifacts which give rise to undesirable visual patterns (e.g., blocking). A large number of approaches have been proposed in literature to reduce the undesirable effects of image compression at post-processing stage [21–23]. Some of them perform a post-filtering in shifted windows of image blocks analyzing the DCT or Wavelet domain during the smoothing procedure. The reduction of compression artifacts at post-processing stage is important to retain the benefits of the compression (for instance, lower transmission and storage costs). The big challenge is to obtain the best results in terms of standard quality measures with the smallest number of visual errors.

In this paper we present the results obtained employing the Structure Sparse Coding Model Selection (SSMS) [16] to restore compressed noisy images. SSMS has been demonstrated to be a powerful tool for different imaging issues (e.g., image denoising, deblurring and inpainting). Here we consider the problem of restoring gray and color images which have been altered by an additive Gaussian noise and further compressed with the lossy compression JPEG algorithm. The underlying ideas, that we start to address in this paper, is related to the fact that in presence of complex or unknown imaging pipelines, where different factors

---

<sup>1</sup> *Demosaicking* can be considered as a special case of the inpainting problem with regular subsampling on a specific uniform grid for each color channel, contaminated by an additive noise due to sensors characteristics.

contribute to the degradation of the original signal (e.g., CFA subsampling, noise, compression, etc.), sparse coding methods could be adopted to restore the original signals.

Experimental results performed on the standard Kodak dataset<sup>2</sup> show that the employed framework makes possible to recover information with a significant margin also in presence of high noise coupled with high compression factor, even though the original framework is not tuned for the specific task of compression. Quantitative and qualitative results pointed out that SSMS is able to perform both denoising and reduction of the blocking artifacts introduced by compression, by demonstrating the promise of sparse coding methods in the context under consideration.

The remainder of the paper is organized as follows: Section 2 introduces the sparse coding concepts, whereas Section 3 presents the SSMS framework for denoising. Section 4 reports the experiments and discusses the results obtained exploiting SSMS to restore compressed noisy images. Section 5 concludes the paper with avenues for further research.

## 2 Sparse Coding for Image Enhancement and Restoration

Sparse coding has emerged as powerful paradigm to describe signals based on the sparsity and redundancy of their representations [17–19]. For signals of a class  $\Gamma \subset \mathbb{R}^N$ , this model suggests the existence of a dictionary  $\mathbf{D} \in \mathbb{R}^{N \times K}$  which contains  $K$  prototype signals ( $|\Gamma| \gg K \geq N$ ), also referred as atoms. The model assumes that for any signal  $\mathbf{I} \in \Gamma$  there exists a sparse linear combination of atoms from  $\mathbf{D}$  that approximates it well. When  $K > N$  the dictionary is said to be redundant or overcomplete. The dictionary employed to sparsely represent the signals is usually learned from a dataset [19].

The sparse coding model has been successfully exploited in the contexts of image enhancement and restoration [9–16], where it is considered the state-of-the-art in terms of both quantitative and qualitative results. In these contexts, images are decomposed into overlapping patches  $\mathbf{I} \in \Gamma$  of size  $\sqrt{N} \times \sqrt{N}$ . A patch is assumed to be sparsely represented in an overcomplete dictionary  $\mathbf{D} = \{\mathbf{d}_1, \dots, \mathbf{d}_K\} \subset \Gamma$ :

$$\mathbf{I} = \mathbf{I}_\Lambda + \mathbf{e} = \sum_{m=1}^M a_m \mathbf{d}_m^\Lambda + \mathbf{e} \quad (2)$$

where  $\mathbf{d}_m^\Lambda \in \Lambda \subseteq \mathbf{D}$ ,  $M = |\Lambda| \leq K$  and the approximation error  $\|\mathbf{e}\|^2 \ll \|\mathbf{I}\|^2$ . A sparse approximation  $\tilde{\mathbf{I}} = \sum_{m=1}^M \tilde{a}_m \mathbf{d}_m^\Lambda$  of  $\mathbf{I}$  is obtained with a basis pursuit algorithm which minimizing a Lagrangian penalized by a sparse  $l^1$  norm:

$$\tilde{\mathbf{a}} = \arg \min_{\mathbf{a}} \left\| \mathbf{I} - \sum_{k=1}^K a_k \mathbf{d}_k \right\|^2 + \lambda \|\mathbf{a}\|_1. \quad (3)$$

<sup>2</sup> The Kodak dataset is available at the <http://r0k.us/graphics/kodak/>

In a typical inverse problem the aim is to estimate  $\mathbf{I}$  from a degraded version

$$\mathbf{J} = \mathbf{U}\mathbf{I} + \mathbf{w} \quad (4)$$

which has been obtained through a non-invertible linear degradation operator  $\mathbf{U}$ , and further altered by an additive noise  $\mathbf{w}$ . Taking into account the Equation (2) the degraded image  $\mathbf{J}$  can be written as

$$\mathbf{J} = \sum_{m=1}^M a_m \mathbf{U}\mathbf{d}_m^\Lambda + \mathbf{e}', \quad (5)$$

with  $\mathbf{e}' = \mathbf{U}\mathbf{e} + \mathbf{w}$ . This means that the degraded image  $\mathbf{J}$  is well approximated by using the same coefficients  $\mathbf{a}$  that are useful to sparsely approximate  $\mathbf{I}$  in Equation (3) together with the transformed dictionary  $\mathbf{UD} = \{\mathbf{U}\mathbf{d}_1, \dots, \mathbf{U}\mathbf{d}_K\}$ . The inverse problem of estimating an approximation of  $\mathbf{I}$  from the degraded version  $\mathbf{J}$  is hence solved by replacing the original dictionary  $\mathbf{D}$  with the transformed one  $\mathbf{UD}$  in the Equation (3).

### 3 Structured Sparse Model Selection

The degree of freedom in selecting the few atoms of the dictionary used to approximate  $\mathbf{I}$  is exponentially large. This fact leads to unstable signal estimation. The Structured Sparse Model Selection (SSMS) put “structure” in sparsity to stabilize the estimation [16]. SSMS is defined with a dictionary  $\mathbf{D}$  composed by  $H$  sub-dictionaries  $\mathbf{B}^1, \dots, \mathbf{B}^H$ , each being an orthogonal basis. An image patch  $\mathbf{I} \in \mathbb{R}^N$  is assumed to be well approximated in one of these sub-dictionaries:

$$\mathbf{I} = \sum_{m=1}^M \langle \mathbf{I}, \mathbf{b}_m^{h_0} \rangle \mathbf{b}_m^{h_0} + \mathbf{e}^{h_0}, \quad (6)$$

where  $h_0$  is the index of the sub-dictionary that best approximate  $\mathbf{I}$  in Equation (6). The best basis  $\mathbf{B}^{h_0}$  is selected by maximizing the projection energy on  $\mathbf{B}^h = \{\mathbf{b}_1^h, \mathbf{b}_2^h, \dots, \mathbf{b}_M^h\}$  over all the orthogonal bases  $\mathbf{B}^h \in \mathbf{D}$ :

$$h_0 = \arg \min_h \sum_{m=1}^M |\langle \mathbf{I}, \mathbf{b}_m^h \rangle|^2. \quad (7)$$

In this model the sub-dictionaries are initialized with Principal Component Analysis (PCA) over syntetic edge patterns of size  $\sqrt{N} \times \sqrt{N}$ . The edge patterns are grouped taking into account various orientations (Figure 1). For each orientation, the PCA over the relative syntetic edge patterns is computed and a basis is obtained. For each basis only the first  $\sqrt{N}$  eigenvectors are retained, whereas the others are discarded due their negligible corresponding eigenvalues. The first eigenvector is replaced with the DC component.



**Fig. 1.** Synthetic edge patterns with orientation  $30^\circ$

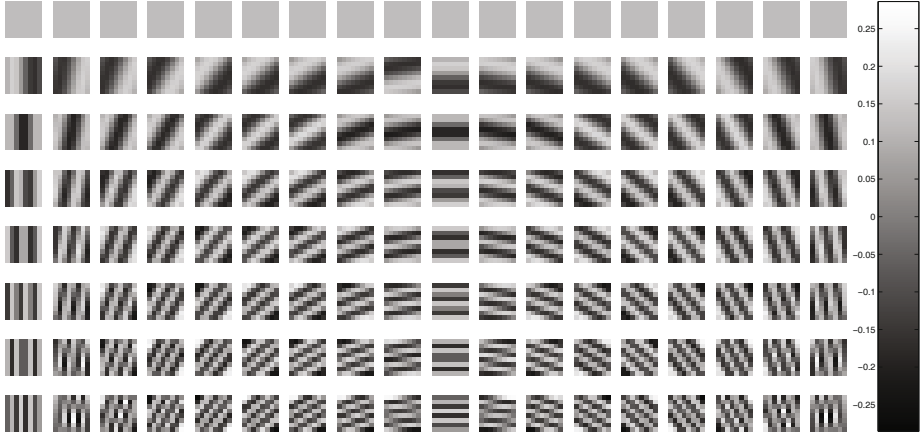


**Fig. 2.** The dictionary obtained through PCA on synthetic edge patterns grouped taking into account different orientations. Columns correspond to a specific sub-dictionary (one for each orientation). Each basis is composed by eight atoms (rows). The fourth column is related the basis obtained considering the synthetic edge patterns in Figure 1.

Figure 2 shows the sub-dictionaries computed on the synthetic edge patterns of size  $8 \times 8$  and 18 different orientations (from  $0^\circ$  to  $170^\circ$  with a step of  $10^\circ$ ). The sub-dictionaries are further adapted to the image of interest by applying the PCAs over the image patches, grouped following the model selection. First, the SSMS assign a model  $h$  to each image patch, then each basis  $\mathbf{B}^h$  is adapted to the image by recalculating the PCA with all the image patch that have been assigned to the model  $h$ .

In case of denoising task, where images are degraded with Gaussian noise  $\mathbf{w}$  of variance  $\sigma^2$ , the aim is to estimate  $\mathbf{I}$  from the degraded patch  $\mathbf{J} = \mathbf{I} + \mathbf{w}$ . The final patch approximation computed by SSMS model is obtained with a thresholding estimator in the best basis  $\mathbf{B}^{h_0}$ :

$$\tilde{\mathbf{I}} = \sum_{\mathbf{b}_m^{h_0} \in \Lambda} \langle \mathbf{J}, \mathbf{b}_m^{h_0} \rangle \mathbf{b}_m^{h_0}. \quad (8)$$

where  $\Lambda = \{\mathbf{b}_m^{h_0} : |\langle \mathbf{J}, \mathbf{b}_m^{h_0} \rangle| > T\}$ .

## 4 Experimental Results

Experiments on restoring compressed noisy images have been carried out with the 24 standard benchmark images of the Kodak database. Each test involved an image of the dataset considered in grayscale or color, corrupted with additive Gaussian noise ( $\sigma = 5, 10, 20$ ), and finally compressed (compression quality = *Uncompressed*, 100, 75, 50, 25, 15) through the JPEG Matlab engine. The SSMS was employed with patches of size  $N = 8 \times 8$ ,  $H = 18$  sub-dictionary computed by considering syntetic edge patterns at different orientations (from  $0^\circ$  to  $170^\circ$  with a step of  $10^\circ$ ), size of each sub-dictionary  $M = 8$ , and threshold as suggested in [16] ( $T = 3\sigma$ ). In practical use, a preliminary noise estimation phase ([25–27]) could help to properly set the threshold  $T$ .

The peak signal-to-noise ratio (PSNR) and the structural similarity index (SSIM) [24] are used as performance measure in our quantitative evaluation. The PSNR is considered to assess the quality of reconstruction of the lossy compressed noisy images, whereas SSIM index is useful to assess the quality taking into account the human eye perception.

Table 1 and Table 2 report the quantitative results considering the images in grayscale. For each couple of parameters ( $\sigma$ , compression quality), the reported PSNR and SSIM values are obtained averaging over the PSNR and SSIM results with respect to the 24 images of the Kodak dataset. Experiments point out that SSMS model leads to recover from 0.5545 dB ( $\sigma = 5$ , compression quality = 15) to 4.9879 dB ( $\sigma = 20$ , compression quality = *Uncompressed*) in terms of PSNR, with a gain from 0.0235 to 0.4299 in terms of SSIM. Visual inspection of the images reported in Figure 5 and Figure 6 is useful to assess the quality of the results. Note that in addition to the significant margin obtained in terms of PSNR and SSIM, visual results show that the model leads to remove some undesirable artifacts introduced by JPEG compression, even though the framework is not tuned for the specific task of compression.

Table 3 and Table 4 report the quantitative results obtained considering the images in the RGB color space. For each combination of parameters (color channel, compression quality and  $\sigma$ ), the PSNR and SSIM values are obtained averaging over the PSNR and SSIM results related the 24 images of the Kodak dataset. The average gain in terms of PSNR and SSIM for each color channel at different  $\sigma$  and compression quality is reported in Figure 3 and Figure 4, whereas in Figure 7 and Figure 8 shown the original images and the restored ones.

Since JPEG compression is performed in YCbCr color domain, we have further tested the performance of SSMS to restore compressed noisy images taking into account that color space (without chromatic subsampling). In Table 5 and Table 6 are reported the results obtained restoring an image belonging to the test dataset under consideration, whereas in Figure 9 is shown a particular of both, the input image and the restored one.

Quantitative and qualitative results confirm that SSMS is able to perform denoising as well as compression artifacts reduction (i.e., deblocking), hence demonstrating the promise of sparse coding methods to restore signals which have been corrupted by different combined non-invertible factors.

**Table 1.** Quantitative evaluation through PSNR measure on the Kodak dataset considering images in grayscale

Average PSNR Gray Images		$\sigma$					
		5		10		20	
		Corrupted	Restored	Corrupted	Restored	Corrupted	Restored
Compression Quality	15	34.0468	34.6012	33.1735	34.4414	30.5417	33.5587
	25	34.8751	35.6358	33.1437	35.1633	30.3355	34.2415
	50	35.7431	37.0212	32.9187	35.9523	29.4379	33.9803
	75	36.4144	38.4877	31.9832	36.5222	29.1156	34.0308
	100	37.1075	40.7517	32.0141	36.9737	29.2979	34.2741
	Uncompressed	37.1645	40.7581	32.0392	36.9838	29.3047	34.2926

**Table 2.** Quantitative evaluation through SSIM measure on the Kodak dataset considering images in grayscale

Average SSIM Gray Images		$\sigma$					
		5		10		20	
		Corrupted	Restored	Corrupted	Restored	Corrupted	Restored
Compression Quality	15	0.8118	0.8352	0.7647	0.8256	0.5407	0.7812
	25	0.8498	0.8749	0.7512	0.8533	0.5687	0.8841
	50	0.8703	0.9098	0.7298	0.8794	0.4190	0.8041
	75	0.8766	0.9326	0.6627	0.8930	0.3779	0.8077
	100	0.8617	0.9526	0.6573	0.9018	0.4022	0.8186
	Uncompressed	0.8630	0.9524	0.6585	0.9017	0.4027	0.8187

**Table 3.** Quantitative evaluation through PSNR measure on the Kodak dataset considering images in the RGB color space

Average PSNR - Channel R		$\sigma$					
		5		10		20	
		Corrupted	Restored	Corrupted	Restored	Corrupted	Restored
Compression Quality	15	32.9902	33.3342	32.7338	33.3179	31.5153	32.8581
	25	34.2075	34.6793	33.6011	34.4384	31.4757	33.4783
	50	35.4551	36.1144	34.0996	35.4205	30.9785	33.7740
	75	36.6877	37.6297	34.0933	36.1304	30.2216	33.9218
	100	39.4043	40.5143	34.1726	36.7819	30.3628	34.0484
	Uncompressed	37.1565	40.6088	32.0294	36.8196	29.2926	34.0492

Average PSNR - Channel G		$\sigma$					
		5		10		20	
		Corrupted	Restored	Corrupted	Restored	Corrupted	Restored
Compression Quality	15	33.6942	34.1499	33.3616	34.0998	31.8656	33.4347
	25	34.7088	35.2838	34.0181	34.9745	31.6331	33.7891
	50	36.8089	36.8430	34.4845	35.9155	31.1180	34.0652
	75	37.3821	38.4397	34.4313	36.5933	30.2989	34.1409
	100	39.7078	40.9313	34.1405	36.9259	30.3353	34.1864
	Uncompressed	37.1648	40.6397	32.0526	36.8594	29.3193	34.1325

Average PSNR - Channel B		$\sigma$					
		5		10		20	
		Corrupted	Restored	Corrupted	Restored	Corrupted	Restored
Compression Quality	15	32.8844	33.2351	32.7255	33.3686	31.7672	33.3061
	25	33.9941	34.4873	33.5374	34.4881	31.7236	34.0112
	50	35.2433	35.9493	34.0432	35.5168	31.2101	34.3547
	75	36.5143	37.5120	34.1305	36.3551	30.4399	34.5442
	100	39.3584	40.4643	34.3871	37.0467	30.6662	34.6490
	Uncompressed	37.1969	40.6160	32.0970	36.9827	29.3793	34.5623

**Table 4.** Quantitative evaluation through SSIM measure on the Kodak dataset considering images in the RGB color space

Average SSIM - Channel R		$\sigma$					
		5		10		20	
		Corrupted	Restored	Corrupted	Restored	Corrupted	Restored
Compression Quality	15	0.7953	0.8155	0.7835	0.8106	0.6831	0.7757
	25	0.8431	0.8604	0.8119	0.8447	0.6556	0.7943
	50	0.8836	0.9009	0.8194	0.8743	0.6102	0.8085
	75	0.9059	0.9270	0.8059	0.8917	0.5334	0.8148
	100	0.9222	0.9527	0.7828	0.9013	0.5454	0.8173
	Uncompressed	0.8680	0.9528	0.6663	0.9028	0.4097	0.8196

Average SSIM - Channel G		$\sigma$					
		5		10		20	
		Corrupted	Restored	Corrupted	Restored	Corrupted	Restored
Compression Quality	15	0.8096	0.8306	0.7974	0.8249	0.6926	0.7859
	25	0.8552	0.8727	0.8228	0.8555	0.6619	0.8010
	50	0.8935	0.9103	0.8273	0.8816	0.6141	0.8126
	75	0.9139	0.9341	0.8117	0.8967	0.5347	0.8166
	100	0.9212	0.9533	0.7759	0.9010	0.5348	0.8172
	Uncompressed	0.8665	0.9523	0.6641	0.9018	0.4089	0.8188

Average SSIM - Channel B		$\sigma$					
		5		10		20	
		Corrupted	Restored	Corrupted	Restored	Corrupted	Restored
Compression Quality	15	0.7733	0.7955	0.7614	0.7927	0.6610	0.7622
	25	0.8233	0.8434	0.7916	0.8304	0.6364	0.7828
	50	0.8669	0.8872	0.8022	0.8624	0.5931	0.7966
	75	0.8917	0.9157	0.7907	0.8811	0.5185	0.8014
	100	0.9164	0.9449	0.7761	0.8896	0.5373	0.7992
	Uncompressed	0.8604	0.9458	0.6514	0.8901	0.3949	0.8009

**Table 5.** Average channels' PSNR obtained by considering the image in the YCbCr color space

Average Channels' PSNR (Kodim04)		$\sigma$					
		5		10		20	
		Corrupted	Restored	Corrupted	Restored	Corrupted	Restored
Compression Quality	15	34.1606	34.8368	33.9226	35.0148	32.4425	34.5508
	25	35.6912	36.4566	34.9614	36.2366	32.1483	35.2412
	50	37.2455	38.2577	35.3904	37.5269	31.4054	35.7042
	75	38.4669	39.9343	35.0356	38.2294	30.4014	35.9062
	100	39.7016	42.5318	34.3084	38.9809	30.4972	36.1308

**Table 6.** Average channels' SSIM obtained by considering the image in the YCbCr color space

Average Channels' SSIM (Kodim04)		$\sigma$					
		5		10		20	
		Corrupted	Restored	Corrupted	Restored	Corrupted	Restored
Compression Quality	15	0.8620	0.8897	0.8476	0.8920	0.7175	0.8639
	25	0.8976	0.9198	0.8596	0.9123	0.6586	0.8790
	50	0.9195	0.9426	0.8382	0.9294	0.5883	0.8904
	75	0.9249	0.9557	0.8019	0.9358	0.4937	0.8927
	100	0.9071	0.9681	0.7476	0.9417	0.5007	0.8960

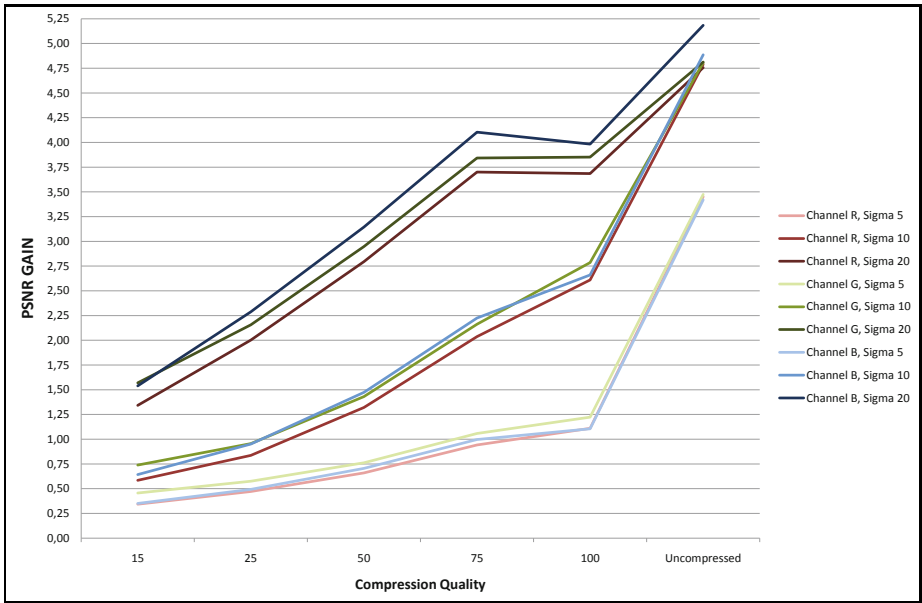


**Fig. 3.** Average gain in terms of PSNR considering the Kodak dataset in the RGB color space

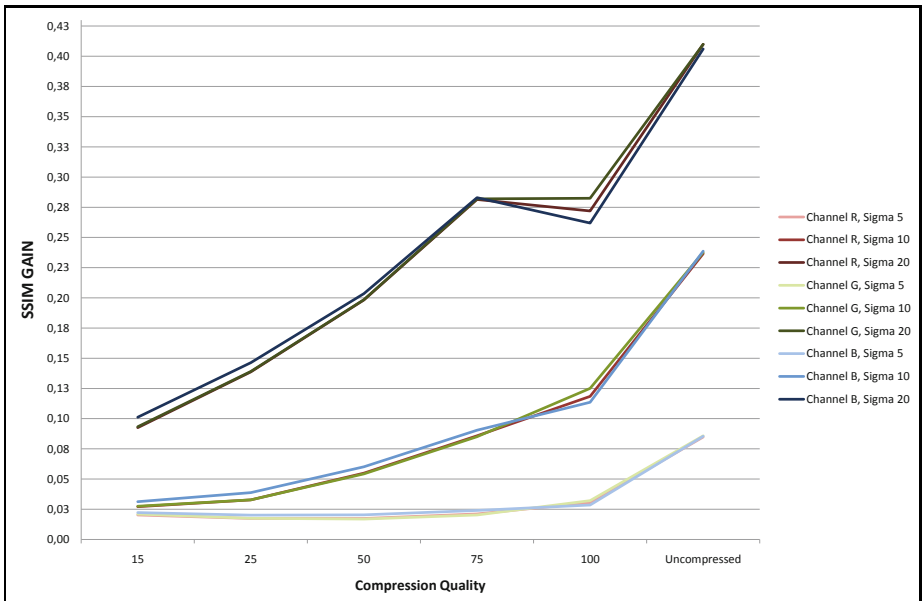


**Fig. 4.** Average gain in terms of SSIM considering the Kodak dataset in the RGB color space

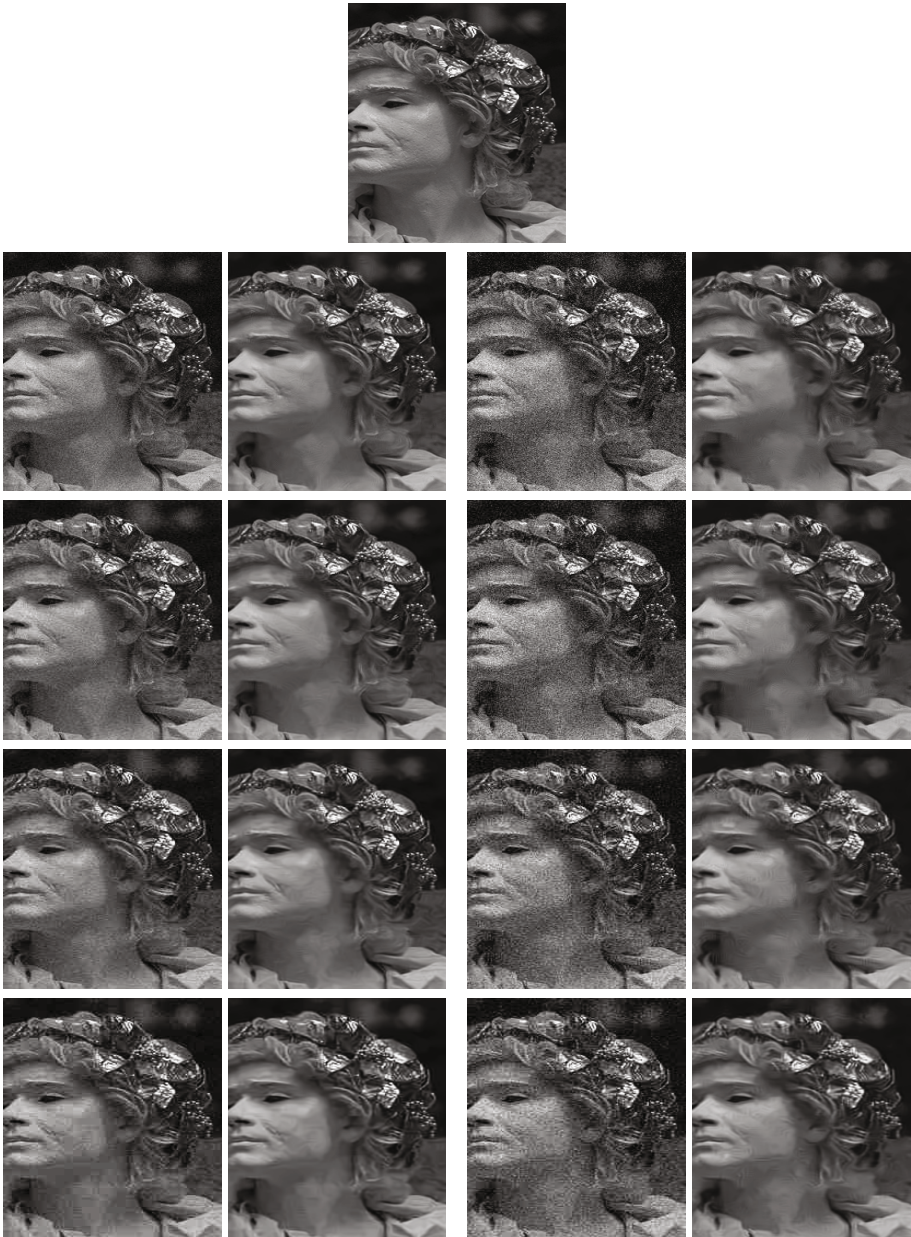


**Fig. 5.** Qualitative evaluation on grayscale images. The original image is shown at the top. Images altered by an additive Gaussian noise are shown in the odd columns (from left to right:  $\sigma = 10, 20$ ), whereas even columns correspond to the restored images. Rows are related the compression quality applied to the noisy image (from top to bottom: 75, 50, 25, 15). The details are better seen by zooming on a computer screen.

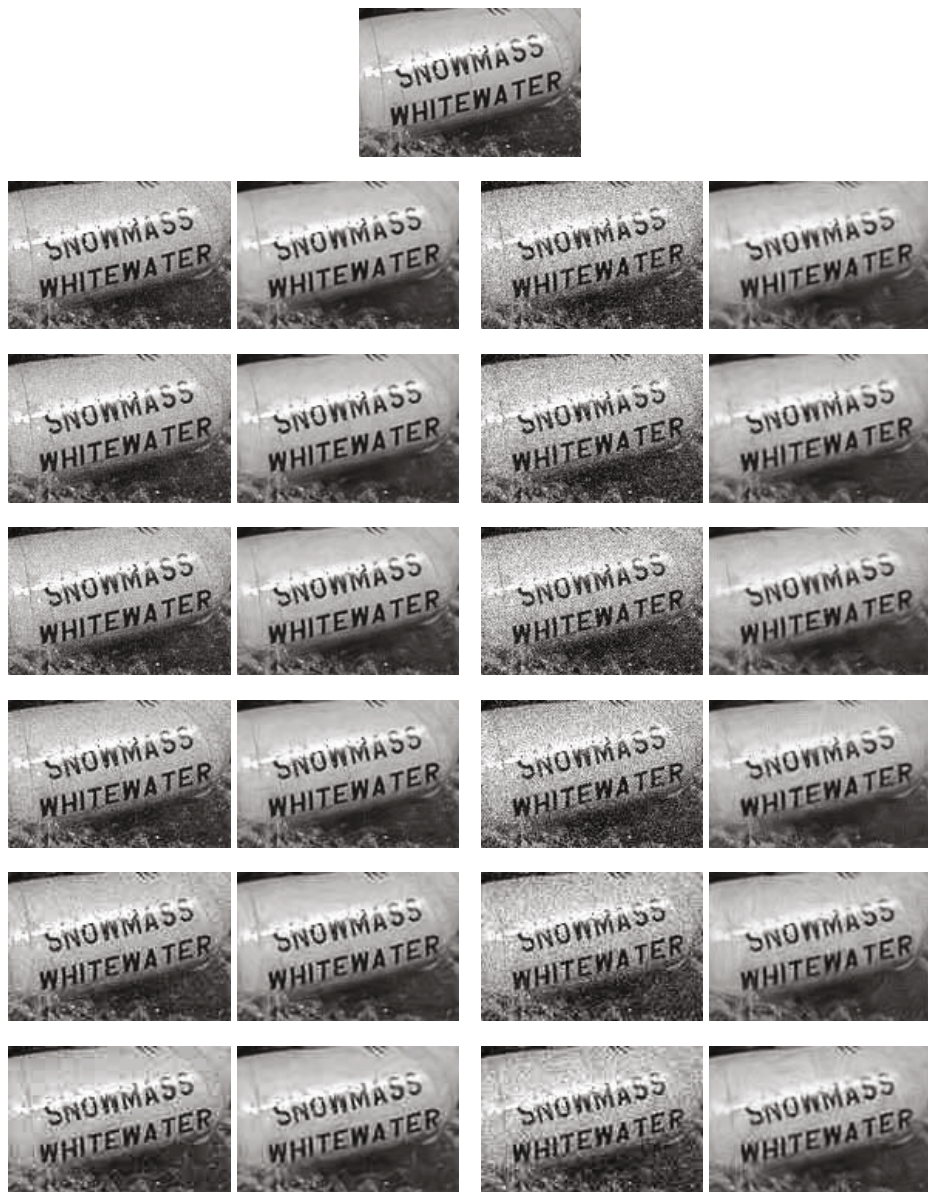


**Fig. 6.** Qualitative evaluation on grayscale images. The original image is shown at the top. Images altered by an additive Gaussian noise are shown in the odd columns (from left to right:  $\sigma = 10, 20$ ), whereas even columns correspond to the restored images. Rows are related the compression quality applied to the noisy image (from top to bottom: *Uncompressed*, 100, 75, 50, 25, 15). The details are better seen by zooming on a computer screen.

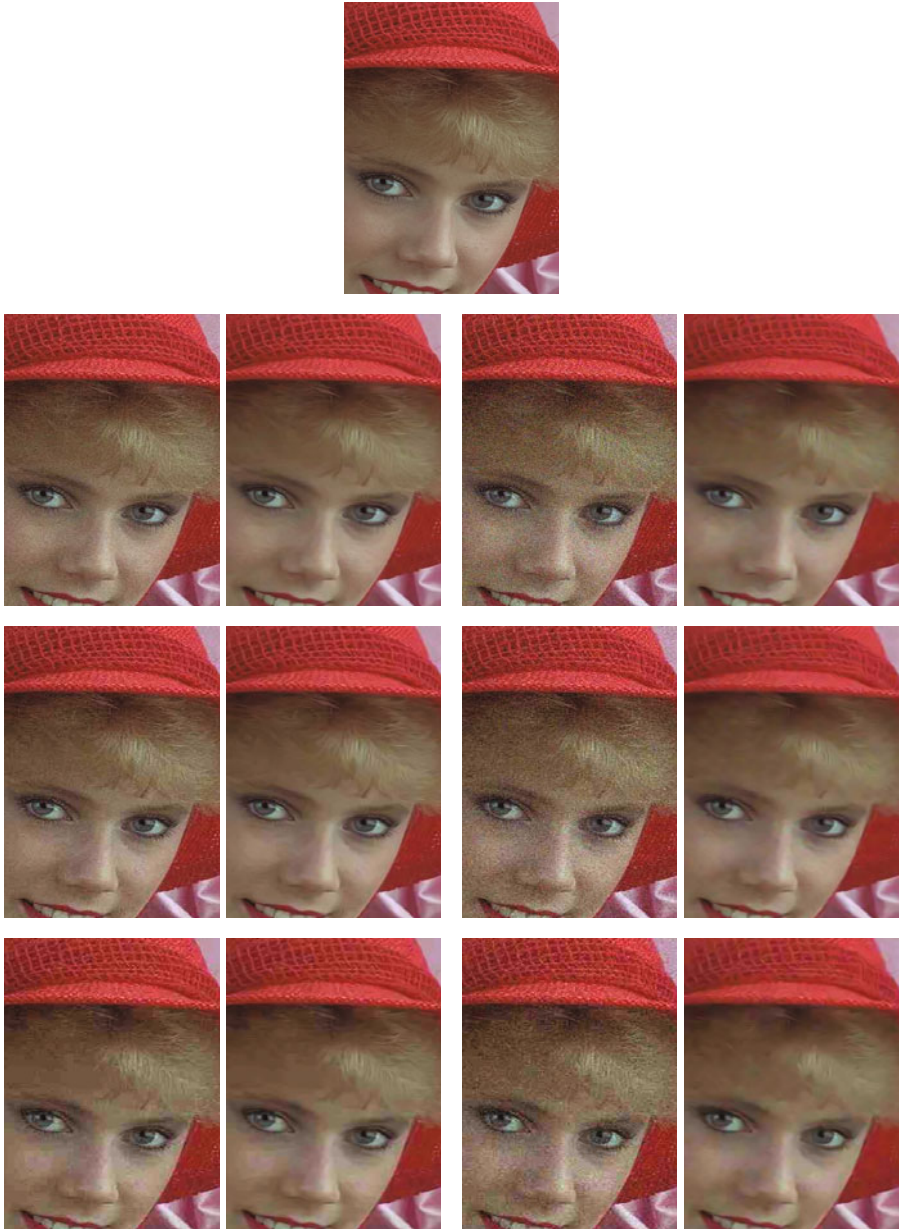


**Fig. 7.** Qualitative evaluation on RGB images. The original image is shown at the top. Images altered by an additive Gaussian noise are shown in the odd columns (from left to right:  $\sigma = 10, 20$ ), whereas even columns correspond to the restored images. Rows are related the compression quality applied to the noisy image (from top to bottom: 50, 25, 15). The details are better seen by zooming on a computer screen.



**Fig. 8.** Qualitative evaluation on RGB images. Images altered by an additive Gaussian noise are shown in the odd columns (from left to right:  $\sigma = 10, 20$ ), whereas even columns correspond to the restored images. Rows are related the compression quality applied to the noisy image (from top to bottom: 50, 25). The details are better seen by zooming on a computer screen.



**Fig. 9.** Qualitative evaluation on YCbCr images. Left: corrupted image ( $\sigma = 20$ , Compression Quality = 50). Right: restored image. The details are better seen by zooming on a computer screen.

## 5 Conclusion and Future Works

Sparse Coding has received considerable attention in recent years as model useful in different imaging problems. In this paper we have considered the problem of restoring information from lossy compressed noisy images by employing the Structured Sparse Model Selection (SSMS) approach. Although the method was not tuned for the specific task of compression, the experiments have shown that it is able to recover significant information obtaining good quantitative and qualitative performances. These preliminary results lead to push our future research in studying sparse coding methods which take into account the compression operator in modeling the representation of the image. Ad-hoc quality measures to assess the deblocking properties [28] should be taken into account in future works.

## References

1. Bertalmío, M., Sapiro, G., Caselles, V., Ballester, C.: Image Inpainting. In: SIGGRAPH (2000)
2. Li, X., Orchard, M.T.: New edge-directed interpolation. *IEEE Transactions on Image Processing* 10(10), 1521–1527 (2001)
3. Battiato, S., Gallo, G., Stanco, F.: A Locally-Adaptive Zooming Algorithm for Digital Images. *Image Vision and Computing Journal* 11(20), 805–812 (2002)
4. Buades, A., Coll, B., Morel, J.-M.: A Non-Local Algorithm for Image Denoising. In: *IEEE Computer Society Conference on Computer Vision and Pattern Recognition* (2005)
5. Buades, A., Coll, B., Morel, J.M.: A review of image denoising algorithms, with a new one. *Multiscale Modeling and Simulation* 4(2), 490–530 (2006)
6. Battiato, S., Bosco, A., Bruna, A.R., Rizzo, R.: Noise Reduction for CFA Image Sensors Exploiting HVS behavior. *Sensors Journal - MDPI Open Access - Special Issue on Integrated High-Performance Imagers* 3(9), 1692–1713 (2009)
7. Joshi, N., Zitnick, C.L., Szeliski, R., Kriegman, D.J.: Image deblurring and denoising using color priors. In: *Computer Vision and Pattern Recognition* (2009)
8. Battiato, S., Guarnera, M., Messina, G., Tomaselli, V.: Recent patents on color demosaicing. *Recent Patents on Computer Science* 1(2), 194–207 (2008)
9. Aharon, M., Elad, M., Bruckstein, A.: K-SVD: An algorithm for designing over-complete dictionaries for sparse representation. *IEEE Transaction on Signal Processing* 54(11), 4311–4322 (2006)
10. Elad, M., Aharon, M.: Image denoising via sparse and redundant representations over learned dictionaries. *IEEE Transactions on Image Processing* 54(12), 3736–3745 (2006)
11. Mairal, J., Elad, M., Sapiro, G.: Sparse representation for color image restoration. *IEEE Transactions on Image Processing* 17(1), 53–69 (2008)
12. Mairal, J., Bach, F., Ponce, J., Sapiro, G., Zisserman, A.: Discriminative Learned Dictionaries for Local Image Analysis. In: *IEEE International Conference on Computer Vision and Pattern Recognition* (2008)
13. Mairal, J., Bach, F., Ponce, J., Sapiro, G., Zisserman, A.: Non-local sparse models for image restoration. In: *International Conference on Computer Vision* (2009)

14. Lou, Y., Bertozzi, A., Soatto, S.: Direct sparse deblurring. Technical Report, CAM-UCLA (2009)
15. Fadili, M.J., Starck, J.L., Murtagh, F.: Inpainting and zooming using sparse representations. *The Computer Journal* 52(1) (2009)
16. Yu, G., Sapiro, G., Mallat, S.: Image Modeling and Enhancement via Structured Sparse Model Selection. In: *IEEE International Conference on Image Processing* (2010)
17. Olshausen, B.A., Field, D.J.: Sparse coding with an overcomplete basis set: A strategy employed by V1? *Vision Research* 37, 3311–3325 (1997)
18. Olshausen, B.A., Field, D.J.: Sparse Coding of Sensory Inputs. *Current Opinion in Neurobiology* 14, 481–487 (2004)
19. Mairal, J., Bach, F., Ponce, J., Sapiro, G.: Online dictionary learning for sparse coding. In: *International Conference on Machine Learning* (2009)
20. Wallace, G.K.: The JPEG still picture compression standard. *Communications of the ACM* 34(4) (1991)
21. Zhai, G., Zhang, W., Yang, X., Lin, W.: Efficient Image Deblocking Based on Post filtering in Shifted Windows. *IEEE Transactions on Circuits and Systems for Video Technology* 18(1), 122–126 (2008)
22. Zhai, G., Zhang, W., Yang, X., Lin, W., Xu, Y.: Efficient Deblocking With Coefficient Regularization, Shape-Adaptive Filtering, and Quantization Constraint. *IEEE Transactions on Multimedia* 10(5), 735–745 (2008)
23. Kim, J.: Adaptive Blocking Artifact Reduction using Wavelet-Based Block Analysis. *IEEE Transactions on Consumer Electronics* (55), 2 (2009)
24. Wang, Z., Bovik, A.C., Sheikh, H.R., Simoncelli, E.P.: Image quality assessment: From error visibility to structural similarity. *IEEE Transactions on Image Processing* 13(4), 600–612 (2004)
25. Foi, A., Trimeche, M., Katkovnik, V., Egiazarian, K.O.: Practical Poissonian-Gaussian Noise Modeling and Fitting for Single-Image Raw-Data. *IEEE Transactions on Image Processing* 17(10), 1737–1754 (2008)
26. Kim, Y.-H., Lee, J.: Image feature and noise detection based on statistical hypothesis tests and their applications in noise reduction. *IEEE Transactions on Consumer Electronics* 51(4), 1367–1378 (2005)
27. Bosco, A., Bruna, A., Giacalone, D., Battiato, S., Rizzo R.: Signal-Dependent Raw Image Denoising Using Image Sensor Characterization Via Multiple Acquisitions. In: *SPIE Electronic Imaging 2010 - Digital Photography VI* (2010)
28. Yim, C., Bovik, A.: Quality Assessment of De-blocked Images. *IEEE Transaction on Image Processing* 20(1), 88–98 (2011)